Compact Car Regenerative Drive Systems: Electrical or Hydraulic

QUINN LAI
School of Mechanical Engineering
Georgia Institute of Technology

The objective of the research is to address the power density issue of electric hybrids and energy density issue of hydraulic hybrids by designing a drive system. The drive system will utilize new enabling technologies such as the INNAS Floating Cup pump/pump motors and the Toshiba Super Charge Ion Batteries (SCiB). The proposed architecture initially included a hydraulic-electric system, where the high power braking power is absorbed by the hydraulic system while energy is slowly transferred from both the Internal Combustion Engine (ICE) drive train and the hydraulic drive train to the electric accumulator for storage. Simulations were performed to demonstrate the control method for the hydraulic system with in-hub pump motors. Upon preliminary analysis it is concluded that the electric system alone is sufficient. The final design is an electric system that consists of four in-hub motors. Analysis is performed on the system and MATLAB Simulink is used to simulate the full system. It is concluded that the electric system has no need for a frictional braking system if the Toshiba SCiBs were used. The regenerative braking system will be able to provide an energy saving from 25% to 30% under the simulated conditions.

ADVISOR:
WAYNE J. BOOK
School of Mechanical Engineering
Georgia Institute of Technology

INTRODUCTION

With around 247 million on-road vehicles traveling around 3 trillion miles (Highway Statistics, 2009) every year, the efficiency of on-road vehicles are of major concern. As a result, hybrid drive trains which dramatically increase urban driving efficiency of vehicles have been developed and implemented in vehicles. Existing on-the-road hybrids have their secondary regenerative systems (Electric Motors and batteries) installed on their primary drive trains (ICE drive train) to provide the regenerative braking capability. Recently efforts have been put in designing drive train systems that have either hydraulic or electric components as integral parts of the systems. For example, in the Chevy Volt, a series electric hybrid system, the ICE is used to charge the electric accumulator, which in turn drives the electric motor (Introducing Chevrolet, 2009).

Electric hybrid drive trains have been implemented in passenger vehicles while hydraulic hybrids have been implemented in commercial vehicles. Since electric hybrid systems can operate quietly, enhancing passenger comfort, this system is implemented in passenger vehicles. However, current battery technologies in the market prevent high power charging and thus prevent the electric system from replacing frictional brakes. As a result a significant amount of braking energy is lost to the surroundings through heat. Hydraulic hybrids, in contrast, have the ability to capture most of the braking power. However, due to the characteristics of hydraulic components, the hydraulic systems suffer from the accumulator's low energy density; the Noise, Vibration and Harshness (NVH) also significantly affect the driving experience.

In an attempt to address the charging power density challenge faced by Electrical Hybrids and the energy density challenge faced by Hydraulic Hybrids, different drive systems were designed. Braking Power Analysis of the report presents simple braking power analysis as the foundation of further calculations in other parts. The initial approach to solve the problem was to incorporate an electrical system in an existing hydraulic hybrid system. Hydraulic Hybrid Drive System presents the Hydraulic Hybrid system engineering level analysis, and Hydraulic Accumulator Analysis investigates the hydraulic accumulator. It was confirmed that the hydraulic accumulator does not have a sufficient energy density for braking energy capture and therefore electrical accumulators were introduced to capture the access energy. Battery Analysis investigates the electrical accumulators. Upon the completion of Analysis, it was concluded that the electrical system alone is sufficient. As a result, an in-hub motor driven electric drive system (Figure 7) was chosen, and the analysis and simulations are presented in Electrical Systems of the paper.

BRAKING POWER ANALYSIS

Braking power analysis is performed to serve as a foundation for accumulator analysis in Hydraulic Accumulator Analisis and Battery Analysis. Analysis is conducted with an assumption of negligible rolling friction, air drag and other losses. The driving analysis is performed on a mid size passenger sedan, such as a Honda FCX Clarity. The Honda FCX Clarity fuel cell car was selected because the weight of the components in the car closely resembles the weight of the suggested drive system. The assumed vehicle mass is 1625 kg (Honda at the Geneva, 2009). The ECE-15 Driving Schedule is shown in Figure 1.

A 6 second 35 mph to 0 mph deceleration is assumed. The assumed braking slope resembles a rapid urban braking is more rapid than ECE-15 Urban Driving Schedule braking. A rapid 60 mph to 0 mph deceleration is also assumed. Under normal driving conditions, a passenger vehicle will take about 200 ft to decelerate (2009 Driver's Manual, 2009). The deceleration time involved can be obtained using Equation (1) and Equation (2)

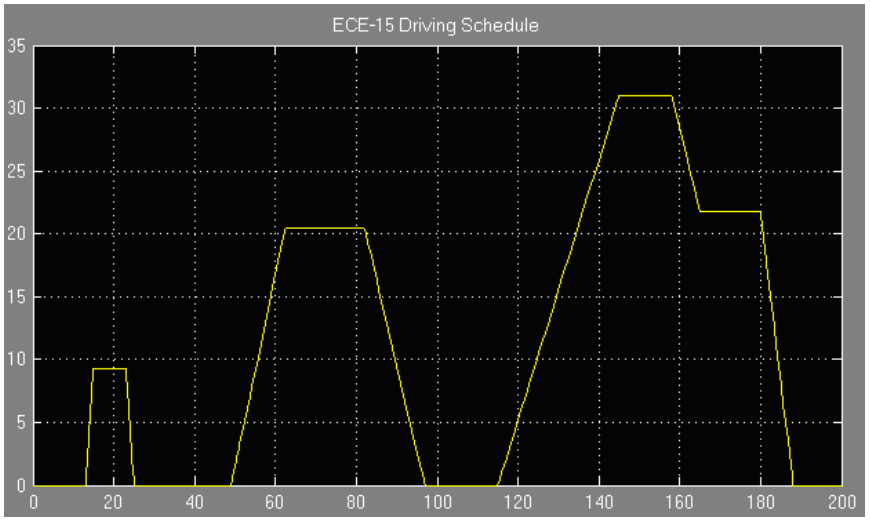

Figure 1. ECE-15 Driving Schedule; x-axis: time (s); y-axis: vehicle velocity (mph).

(1)

$$v_f^{\,2} = v_i^{\,2} + 2as$$

where is the final velocity of the vehicle, is the initial velocity of the vehicle, a is the acceleration of the vehicle, and s is the displacement involved in the acceleration. The time is obtained using Equation (2)

(2)

$$v_f = v_i + at$$

where t is the deceleration time. Using the provided equation, we obtained 11 seconds as the deceleration time. The energy dissipated can be obtained using Equation (3)

(3)

$$KE = \frac{1}{2}mv^2$$

where KE is the kinetic energy of the vehicle, m is the mass of the vehicle, and v is the velocity of the vehicle. The braking power can then be determined using Equation (4)

(4)

$$P = \frac{d(KE)}{dt} = mv\frac{dv}{dt} = mva$$

where P is the power involved with the braking. The deceleration details calculated are tabulated in Table 1.

HYDRAULIC HYBRID DRIVE SYSTEM

The initial approach to solve the problem was to incorporate an electrical system in an existing hydraulic hybrid system. The selected hydraulic system is the INNAS HyDrid. The architecture of the HyDrid system (Achten, 2007) is presented in Figure 2.

INNAS claimed that 77 Miles Per Gallon (MPG) is possible for the HyDrid system (HyDrid, 2009) because

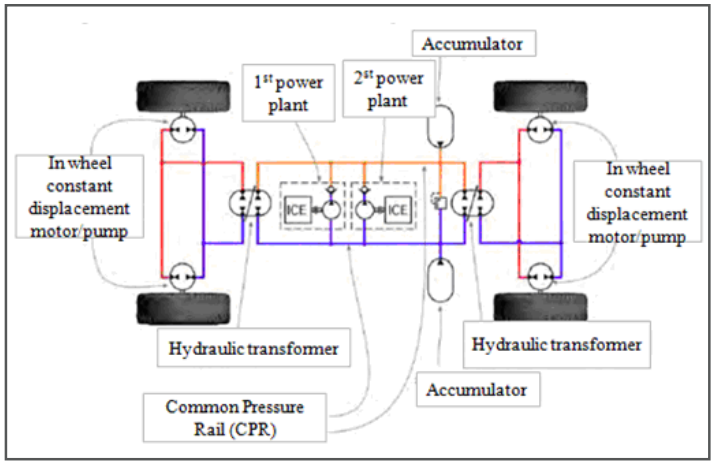

Figure 2. HyDrid Drive system adapted from Achten.

the secondary power plant allows engine off operation, and the Infinitely Variable Transmission (IVT) allows the engine to rotate at optimum RPM for efficiency. The INNAS HyDrid utilizes the INNAS Hydraulic Transformers (IHT) (Achten, 2002) in a Common Pressure Rail (CPR) (Vael & Acten, 2000). The IHT is claimed to have unmatched efficiency due to the Floating Cup Principle that it utilizes. The starting torque efficiency, according to Achten, is up to 90% (Achten, 2002) or above. The control method of the HyDrid is not published; therefore, a possible control method is presented to demonstrate how the IHT functions as an IVT and thus converting the varying pressure from the accumulator into the desired pressure for the in wheel constant displacement motor/pumps. When accelerating, either the pressure accumulator or the ICE will provide the required pressure in the CPR which will in turn be transmitted by the IHT to drive the in-wheel constant displacement motor/pump. The IHT is assumed to be a variable pump coupled with a variable pump/motor. A possible method of controlling the acceleration is to vary the stroke of the variable pump in the IHT while keeping the pump motor stroke and the ICE RPM constant. During braking, the pump (CPR side) stroke is kept constant while the pump motor stroke is varied to charge up the accumulator. The presented control method is presented in Figure 3.

A simulation is performed to demonstrate the control method. The system assumes that the vehicle has a 4 cylinder gasoline engine, a 0.85 volumetric efficiency for variable pump/motor, and a 0.92 volumetric efficiency for constant displacement pumps and inactive pressure accumulators. It is also assumed ideal pipe lines and no force is involved in the varying of the pump stroke. The simulation shows how by varying the IHT pump stroke the vehicle speed can closely follow a desired trajectory with minimal ICE rpm variation. The ICE rpm and the pump stroke variation are shown in Figure 4 and 5

v_i(m/s)	v_f(m/s)	t(s)	Braking Power (kW)
35	0	6	66.0
60	0	11	99.8

Table 1. Deceleration details for the assumed vehicle.

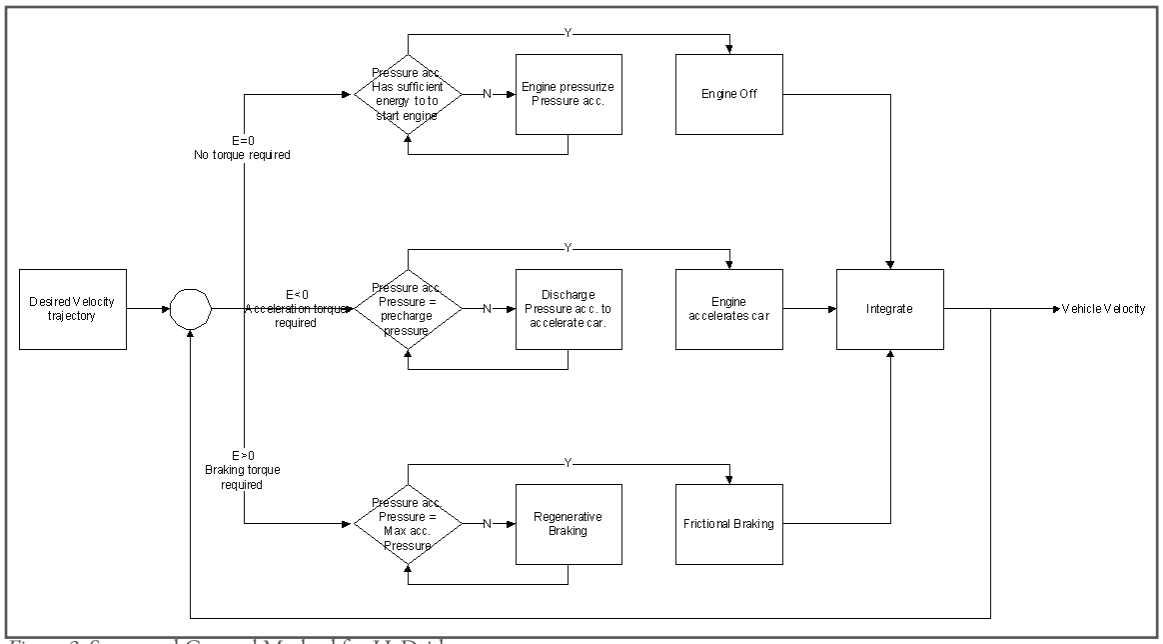

Figure 3. Suggested Control Method for HyDrid system.

respectively. The resulting vehicle velocity is shown in Figure 6.

The simulated vehicle velocity closely matches with the desired velocity trajectory, which is the ECE-15 driving schedule (Figure 1). The simulated velocity trajectory is idealized because of the idealized assumptions made in creating the simulation model. The pressure values provided from the simulation are also observed to be faulty. This simulation's values cannot be used for quantitative purposes. However, it is sufficient for the demonstration of the variation between the stroke of the pump in the IHT and the vehicle velocity.

HYDRAULIC ACCUMULATOR ANALYSIS

The hydraulic accumulator has sufficient power density but a low energy density. An attempt was made to quantify the energy storage capacity of a typical size hydraulic accumulator for a hydraulic hybrid vehicle so that the proposed additional battery pack can be correctly sized. A 38L EATON hydraulic accumulator (Product Literature, 2009) is assumed (Used in CCEFP Test Bed 3: Highway Vehicles). The parameters used for energy calculations are tabulated in Table 2.

Volume (m^3)	0.038
Precharge Pressure (MPa)	10.7
Precharge Nitrogen Volume (m^3)	0.038
Maximum Nitrogen Pressure (MPa)	20.6
Nitrogen Volume at Maximum Pressure (m^3)	0.0176

Table 2. EATON 38 L hydraulic accumulator.

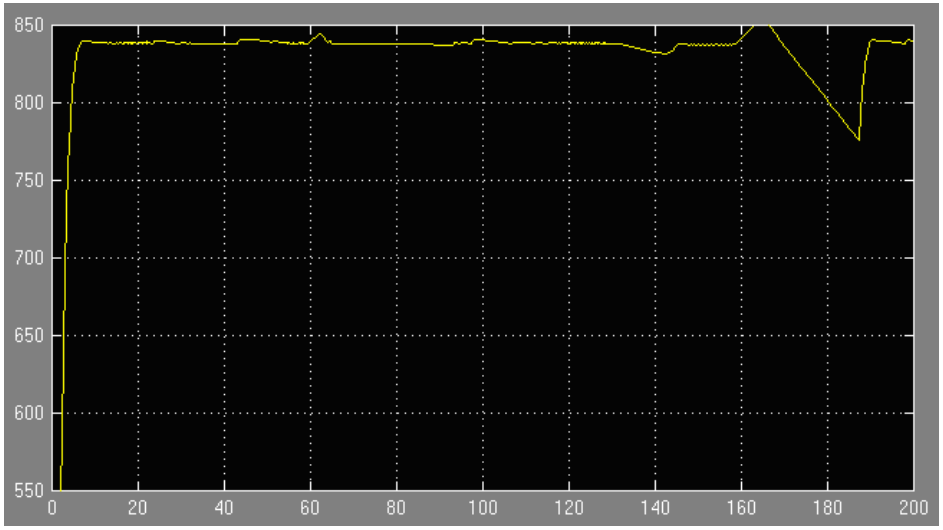

Figure 4. Engine RPM for HyDrid simulation; x-axis: time (s); y-axis: ICE rpm.

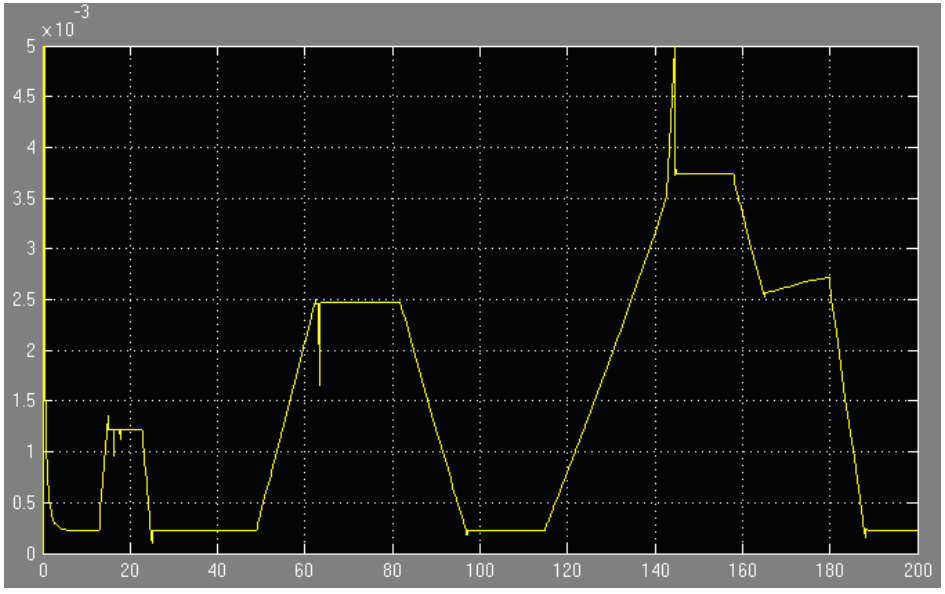

Figure 5. Pump stroke variation for HyDrid simulation; x-axis: time (s); y-axis stroke (m).

The assumed relationship between pressure and volume is shown in Equation (5)

$$pV^n = \text{constant} \quad (5)$$

where p is the pressure of the nitrogen in the accumulator, V is the volume of nitrogen in the accumulator, and n is an empirical constant. Using this relationship, the total energy involved in completely pressurizing or depressurizing the accumulator is shown in Equation (6)

$$W = \frac{p_f V_f - p_i V_i}{1 - n} \quad (6)$$

where is the initial pressure, is the final pressure, is the initial volume, is the final volume, and W is the energy involved. Using Equation (5) and Equation (6) we can calculate the total energy storage of the EATON 38L pressure accumulator, which is 293.6 kJ. Using Equation (3) and assuming a vehicle with the weight of 1625 kg (from Braking Power Analysis), a 38L accumulator is sufficient for the acceleration from 0mph to 42.5mph. It is assumed that no energy is lost due to friction, drag, and inertia changes. As the main purpose of the hydraulic system in a Hydraulic Hybrid is to capture urban braking and to accelerate the car to a velocity where the ICE can be started, 293.6 kJ is sufficient. However, if the vehicle is braking from a speed higher than 42.5 mph, or the duration of braking is long, the hydraulic system will not be able to capture the braking energy.

Therefore an electrical system is introduced to capture the excess energy.

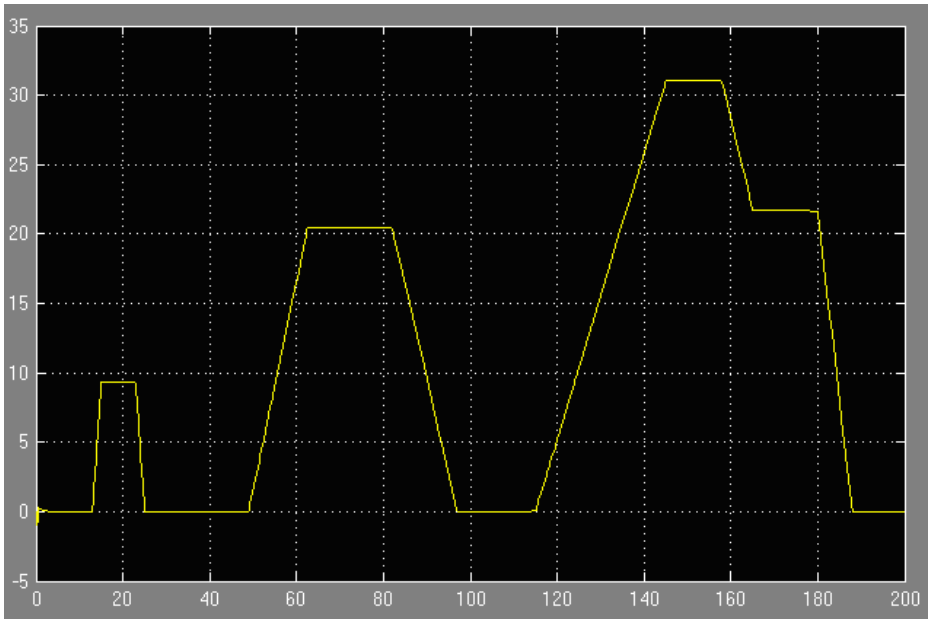

Figure 6. Vehicle velocity variation for HyDrid simulation; x-axis: time (s); y-axis: velocity (mph).

	SCiB Cell	LFP
Nominal Voltage (V)	2.4	3.2
Nominal Capacity (Ah)	4.2	1.1
Size (mm)	approx 62 x 95 x13	d=18, h=65
Weight (g)	approx 150	40
Charging time	90% in 5 min	99% in 30 min

Table 3. Sony LFP and Toshiba SCiB cell spec.

BATTERY ANALYSIS

The batteries are proposed to serve as secondary energy storage which will capture excess energy that cannot be captured by the hydraulic system. The two electric accumulators analyzed are the Sony Olivine-type Lithium Iron Phosphate (LFP) cells (Sony Launches High-Power, 2009) and the Toshiba SCiB cells (Toshiba to Build, 2009). Both cells exhibit impressive recharge cycles and high charging power density. Cell specifications are shown in Table 3.

The charging power density can be obtained using Equation (7).

(7)

$$\text{Charging power density} = \frac{(\%\text{Charge}) \cdot (\text{Energy Density})}{t_{\text{charging}}}$$

where is the charging time for one cell.(fix this sentence) Energy density can be described using Equation (8).

(8)

$$\text{Energy density} = \frac{C \cdot V \cdot 60\ \text{min} \cdot 60\ \text{sec}}{t_{\text{charging}}}$$

where C is the cell capacity in Ah, V is the nominal voltage, and is the mass of one cell. The energy density and charging power density values obtained are tabulated in Table 4.

As shown in Table 4, the Sony LFP outperforms the Toshiba SCiB in terms of energy density by a factor of 1.3, while the SCiB outperforms the LFP in terms of power density by a factor of 3. As the major limitation in Electric Hybrid systems is the charging power density of batteries, the SCiB cell is used for further analysis.

As calculated in Braking Power Analysis, 66.0 kW is the maximum braking power occurred in a 6 second 35mph to 0 mph city braking. Assuming that all the SCiB cells used are arranged in such a way that the power density is equally shared among the cells and ideal electronic components, 90.8 kg of the SCiB cells are required. 90.8 kg of SCiB has a total capacity of 22,000 kJ. According to Braking Power Analysis calculations, each city braking involves 197.7 kJ braking energy, which is 0.9% of the battery pack's capacity. According to Toshiba, the capacity loss after 3,000 cycles of rapid charge and discharge is less than 10% (Toshiba to Build, 2009). Using the assumptions in Braking Power Analysis and assuming that the 10% of capacity loss after 3000 cycles is negligible, we can obtain 334 thousand cycles as an approximate

	SCiB Cell	LFP
Energy Density (kJ/kg)	242	316.8
Charging Power Density (W/kg)	726	198

Table 4. Sony LFP and Toshiba SCiB cell spec (charging power density and energy density).

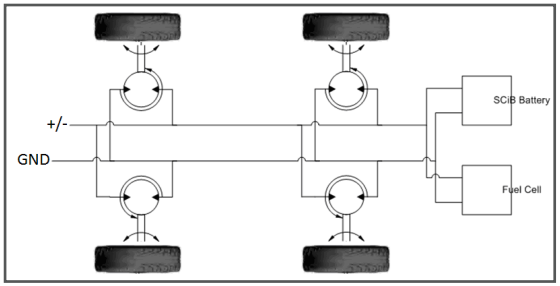

Figure 7. Selected Electric Car architecture.

for the regenerative braking and driving cycles allowed before the capacity of the SCiB drops below 90%. Using the same assumptions we can also find that 137.6 kg of SCiB is sufficient for the maximum charging power involved in the 11 second 60 mph to 0 mph highway accident braking. The weight of the battery pack required is slightly heavier than the 70kg battery pack in a Toyota Prius electric hybrid vehicle.

ELECTRICAL SYSTEMS

As shown in Battery Analysis calculations, the Toshiba SCiBs have a power density that is more than sufficient for regenerative braking. As a result neither the hydraulic system nor the frictional braking system is necessary in an electric vehicle equipped with the Toshiba SCiBs. A mechanical emergency brake should be installed to prevent accidents in case of regenerative braking system failure.

The possible simplest design is a plug in electric or a fuel cell vehicle that has 4 in-hub motors. The simplified system is shown in Figure 7. As shown in the Figure 7, the 4 in-hub wheel motors are directly connected to the wheel. With mechanical components such as the ICE, differentials, and the transmission removed, the vehicle weight can be reduced, and the efficiency of the whole driving train can be increased by at least a factor of 3 (Clean Urban Transport, 2009). Some efficiency values (Achten, 2009; Valøena & Shoesmith, 2009) are provided in Table 5 for comparison. The 4 in-hub motor design also allows the vehicle to enjoy a very small turning radius and other advantages of 4WD vehicles, such as increased traction performance and precision handling. To validate the design, a simulation is done for the system suggested. Because of the mechanical components removed, a lighter car is selected for simulation. The selected vehicle is a Honda Civic, with a vehicle mass of 1246 kg (Complete Specifications, 2009) and a CdA value of 0.682 m2. The air drag of the vehicle can be calculated using Equation (9) (Larminie & Lowry, 2003)

(9)

$$F_{ad} = \frac{1}{2}\rho C_d A v^2$$

where is the drag force, is air density, is the drag coefficient, A is the cross sectional area of the vehicle facing the front, and v is the velocity of the vehicle. The rolling friction of the vehicle can be obtained using Equation (10) (Larminie & Lowry, 2003).

(10)

$$F_{rr} = \mu_{rr} mg$$

	Approx. Efficiency
ICE	20%
Transmission (automatic)	85%
Transmission (manual)	92% to 97%
Differential	90%
Motor	90%
Battery recharge	80% to 90%

Table 5. Efficiency values of integral components of ICE drive train and electric drive train.

where is the rolling friction force, is the rolling friction coefficient, which is assumed to be 0.015 (for radial ply tire) (Larminie & Lowry, 2003), m is the mass of the vehicle, and g is the acceleration due to gravity. As in-hub motor specifications are not readily available, the 4 in-hub motors are assumed to resemble the Tesla Roadster drive train system (2010 Tesla Roadster, 2009), which only involves a motor and a fix gear set with a gear train ratio of 8.28. The 375 V AC motor has a 215kW peak power and 400 Nm of torque. All the parameters, including Equation (9) and Equation (10), are included in the simulation.

The model simulates the vehicle attempting to follow the ECE Driving Schedule shown in Figure 1. The controller assumed is a PID controller with a Kp of 10.4, Ki of 0.546, and a Kd of -0.386 (MATLAB Simulink tuned for 2.06 second response time). The resultant velocity trajectory and the power variation are shown in Figure 8 and Figure 9 respectively

As expected, the power stays below a value of 66kW, and there are negative values in the time versus power plot as deceleration is involved in the ECE 15 Driving Schedule. Because of the losses, the negative peaks that correspond to braking power have a magnitude that is relatively smaller than the positive peaks that correspond to accelerating power. From the simulation, the highest braking power observed is a little over 10 kW, which can easily be fully captured using the 70kg of SCiB battery packs (refer to Battery Analysis for calculations). Simulink scopes are added to the system to observe the energy change with and without regenerative braking systems. The results are shown in Figure 10 and Figure 11.

Comparing Figures 9 and 10, we can observe a 25% energy saving for the system with regenerative braking. Tuning the PID controller can increase the energy savings value up to 30%. Using a better controller has the potential to increase the energy savings value further.

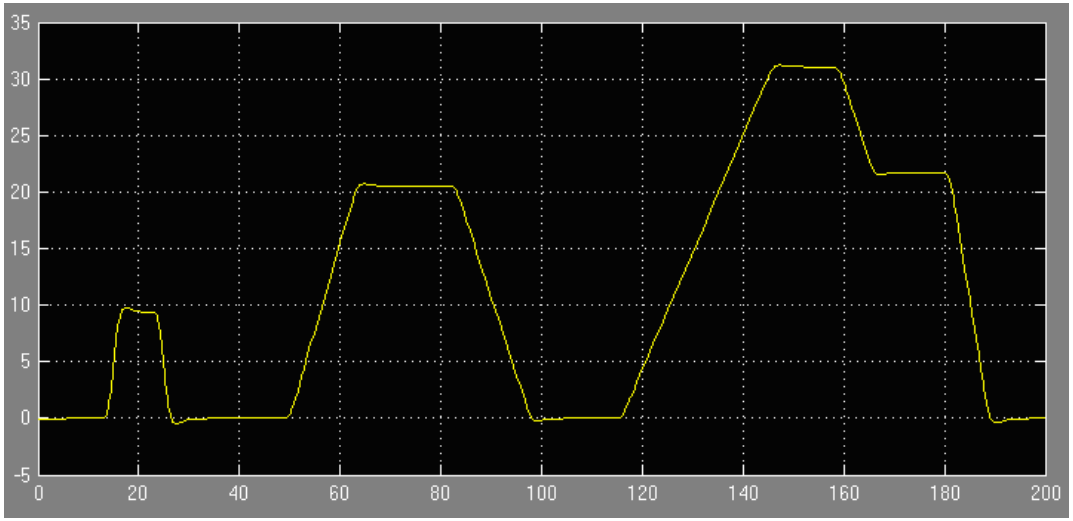

Figure 8. Vehicle Velocity Variation for Electric Drive System; x-axis: time (s); y-axis: velocity (mph).

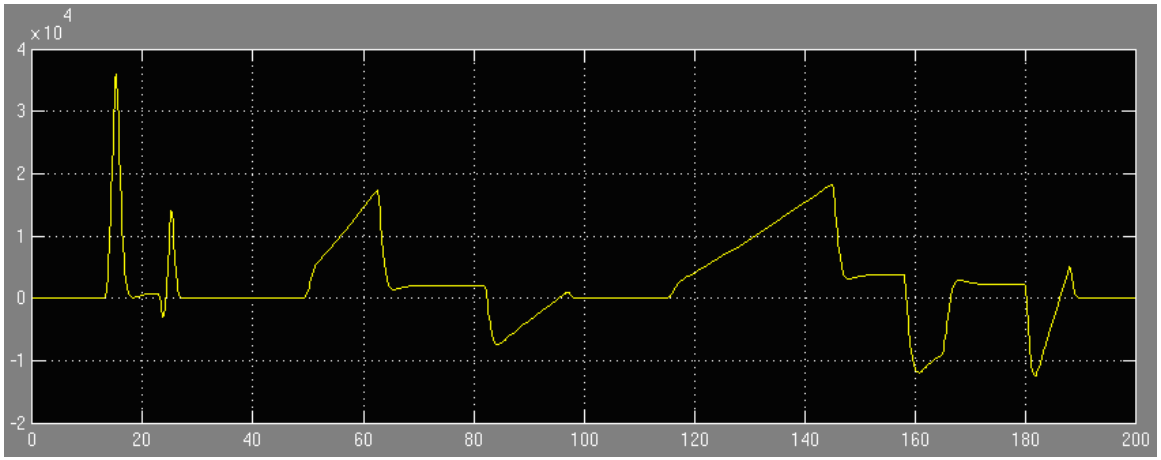

Figure 9. X-axis: time (s); y-axis: power(W) plot for Electric Drive System Simulation.

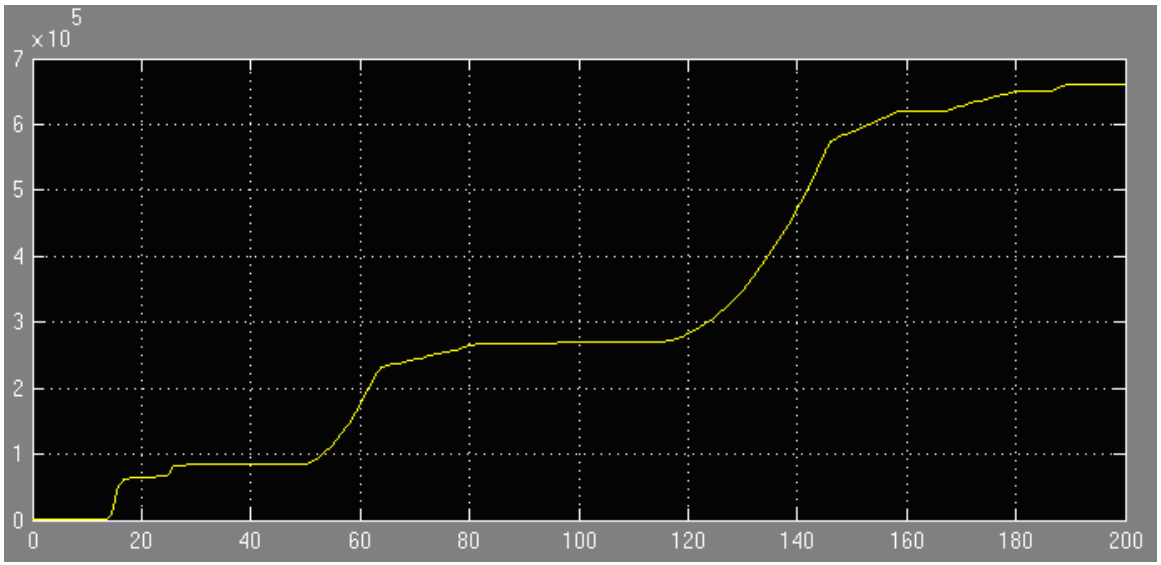

Figure 10. Energy required to complete the ECE 15 driving cycle without regenerative braking; x-axis: time(s); y-axis: energy(J).

RECOMMENDED FUTURE WORK

The hydraulic drive system may deserve a more in depth analysis. If the accumulator energy density can be improved, the hydraulic drive system may be a more environmentally friendly option than its electrical counterparts as the production and disposal of batteries leave detrimental effects to the environment. It is recommended that the simulation model be improved to better model the actual response of the HyDrid system. For the electrical system, efforts should be invested in the research of in-hub motors, which produce significantly less torque than a regular AC motor coupled with an 8.28 to 1 gear ratio gear train. Parameters within the Simulink model should be selected to better represent in-hub motors and the batteries should be modeled with greater detail, as different arrangements of the cells will result in different power density. Losses involved with the electrical components should also be investigated. One challenge that the electric drive system should overcome is the energy density issue of the batteries. The energy density of a battery is significantly lower than gasoline. Efforts should also be invested in technologies related with battery recycling. (this is not your future work)

CONCLUSION

An attempt was made to design a compact car drive system to address the charging power density challenge faced by electric hybrid vehicles and the charging energy density challenge faced by hydraulic hybrid vehicles. The initial approach to solve the problem was to incorporate an electrical system in an existing hydraulic hybrid system. The INNAS HyDrid was used as the foundation architecture for analysis. Simulations were performed to understand the control dynamics of the HyDrid. After performing quantitative analysis on hydraulic accumulators it was confirmed that hydraulic accumulators cannot provide a sufficient energy density for braking

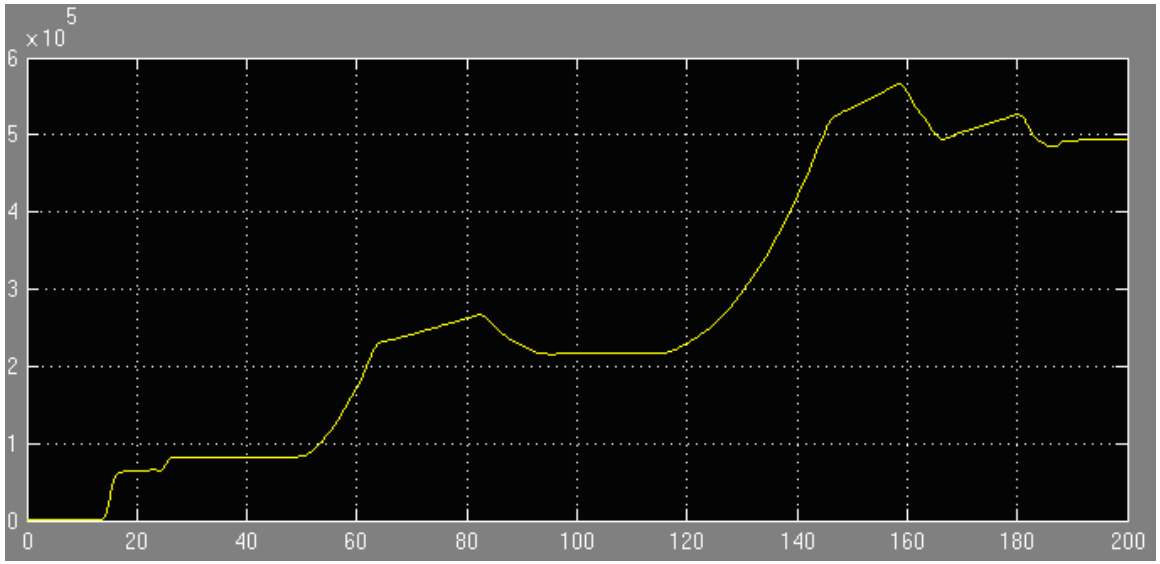

Figure 11. Energy required to complete the ECE driving cycle with regenerative braking; x-axis: time(s); y-axis: energy(J).

energy storage. In one of the intermediate designs, electrical accumulators were introduced into the system to capture excess energy that cannot be captured by the hydraulic system. The Sony LFP and the Toshiba SCiB were considered. The Toshiba SCiB was chosen as a result of its superior charging power density performance. Upon further analysis, it was concluded that the batteries have a sufficient charging power density to capture braking power. It was then suggested that the electric system can fully replace the hydraulic components, the ICE drive train, and the frictional braking system. With the convoluted hybrid system, which consists of a lot of inefficient components replaced by a simple electric only drive train, the vehicle drive train efficiency can be increased. An electrical system is simulated. The simulated models showed energy savings of around 25~30% with regenerative braking. The final drive system design consists of an electric/fuel cell vehicle with four in-hub motors.

REFERENCES

Highway Statistics. (2007). Washington, D.C.: Federal Highway Administration Retrieved from http://www.fhwa.dot.gov/policyinformation/statistics/2007/.

Introducing the Chevrolet Volt. (2010) Retrieved December 5, 2009, from http://www.chevrolet.com/pages/open/default/future/volt.do

Honda at the Geneva Motor Show. Retrieved December 5, 2009, from http://world.honda.com/news/2009/c090303Geneva-Motor-Show/

Larminie, J., & Lowry, J. (2003). Electric Vehicle Technology Explained. Chichester: John Wiley & Sons Ltd.

Driver's Manual. (2009). Government of Georgia. Retrieved from http://www.dds.ga.gov/docs/forms/FullDriversManual.pdf.

Acten, P.A.J. (2007). Changing the Paradigm. Paper presented at the Proc. of the Tenth Scandinavian Int. Conf. on Fluid Power, SICFP'07, Tampere, Finland.

HyDrid. Retrieved December 5, 2009, from http://www.innas.com/HyDrid.html

Achten, P.A.J. (2002). Dedicated design of the hydraulic transformer. Paper presented at the Proc. IFK.3, IFAS Aachen.

Vael, G.E.M., Achten, P.A.J., & Fu, Z. (2000). The Innas Hydraulic Transformer, the Key to the Hydrostatic Common Pressure Rail. Paper presented at the International Off-Highway & Powerplant Congress & Exposition, Milwaukee, WI, USA.

Accumulators Catalog. (2005). In Eaton (Ed.), Vickers.

Sony Launches High-power, Long-life Lithium Ion Secondary Battery Using Olivine-type Lithium Iron Phosphate as the Cathode Material. (2009). News Releases Retrieved December 5, 2009, from http://www.sony.net/SonyInfo/News/Press/200908/09-083E/index.html

Toshiba to Build New SCiB Battery Production Facility. (2008). News Releases Retrieved December 5, 2009, from http://www.toshiba.co.jp/about/press/2008_12/pr2401.htm

Berdichevsky, G., Kelty, K., Straubel, J.B., & Toomre, E. (2006). The Tesla Roadster Battery System. In Tesla Motors (Ed.).
Electric Vehicles. (2009). Retrieved from http://ec.europa.eu/transport/urban/vehicles/road/electric_en.htm.

Valøen, L.O., & Shoesmith, M.I. (2007). The effect of PHEV and HEV duty cycles on battery and battery pack performance. Paper presented at the Plug-in Hybrid Electric Vehicle 2007 Conference, Winnipeg, Manitoba. http://www.pluginhighway.ca/PHEV2007/proceedings/PluginHwy_PHEV2007_PaperReviewed_Valoen.pdf

Complete Specifications. Civic Sedan Retrieved December 5, 2009, from http://automobiles.honda.com/civic-sedan/specifications.aspx

Performance Specifications. (2010). Tesla Roadster Retrieved December 5, 2009, from http://www.teslamotors.com/performance/perf_specs.php